HHS Public Access

Author manuscript

Obesity (Silver Spring). Author manuscript; available in PMC 2014 June 01.

Published in final edited form as:

Obesity (Silver Spring). 2013 December ; 21(12): 2522–2529. doi:10.1002/oby.20378.

In Vivo Multi-Tissue Efficacy of Peroxisome Proliferator-Activated Receptor-γ Therapy on Glucose and Fatty Acid Metabolism in Obese Type 2 Diabetic Rats

Samuel Nemanich[1], **Sudheer Rani**[1], and **Kooresh Shoghi**[1,2,3,*]

[1]Department of Radiology, Washington University in St. Louis, Saint Louis, MO

[2]Department of Biomedical Engineering, Washington University in St. Louis, Saint Louis, MO

[3]Division of Biology and Biomedical Sciences, Washington University in St. Louis, Saint Louis, MO

Abstract

Objective—To identify the disturbances in glucose and lipid metabolism observed in Type 2 Diabetes Mellitus (T2DM), we examined the interaction and contribution of multiple tissues (liver, heart, muscle, and brown adipose tissue) and monitored the effects of the PPARγ agonist rosiglitazone (RGZ) on metabolism in these tissues.

Design and Methods—Rates of [^{18}F]FDG and [^{11}C]Palmitate uptake and utilization in the Zucker Diabetic Fatty (ZDF) rat were quantified using non-invasive positron emission tomography (PET) imaging and quantitative modeling in comparison to lean Zucker rats. Furthermore, we studied two separate groups of RGZ-treated and untreated ZDF rats

Results—Glucose uptake is impaired in ZDF brown fat, muscle, and heart tissues compared to leans, while RGZ treatment increased glucose uptake compared to untreated ZDF rats. Fatty acid (FA) uptake decreased, but FA flux increased in brown fat and skeletal muscle of ZDF rats. RGZ treatment increased uptake of FA in brown fat, but decreased uptake and utilization in liver, muscle and heart.

Conclusion—Our data indicate tissue-specific mechanisms for glucose and FA disposal as well a differential action of insulin-sensitizing drugs to normalize substrate handling and highlight the role that pre-clinical imaging may play in screening drugs for obesity and diabetes.

*Corresponding Author: Kooresh I. Shoghi, Mallinckrodt Institute of Radiology, Washington University School of Medicine, 510 S. Kingshighway Blvd. Campus Box 8225, Saint Louis, MO 63110. Phone: +1-314-362-8990, Fax: +1-314-362-9940, shoghik@wustl.edu.

Conflicts of Interest

The authors have no conflicts of interest to report.

Supplementary Information

The supplementary material contains descriptions of the quantification of the portal vein input function and the equations describing the kinetic modeling of PET data and the definition of the metabolic estimates presented here. In addition, it includes representative fits of kinetic modeling to PET data. The material is available at www.nature.com/obesity.

Keywords

Type 2 Diabetes; Fatty acid metabolism; Small-animal PET imaging; PPARγ therapy

Introduction

Type 2 Diabetes Mellitus (T2DM) is a result of systemic disturbances in metabolism characterized by impaired insulin action in peripheral tissues such as liver, muscle, and adipose tissue (1). Recent epidemiological and experimental evidence suggests that there is a close link between the pathogenesis of obesity and T2DM (2). In general, animal models of obesity and T2DM attempt to recapitulate the phenotype of insulin resistance in T2DM, which involves metabolic disturbances in multiple tissues including liver, muscle, white and brown adipose tissue (BAT), pancreas, among others, and secondary effects on the heart (3).

Skeletal muscle is a major contributor to peripheral glucose disposal, accounting for over 60% of GLUT-mediated glucose uptake. Increased supply and/or decreased oxidation of lipids beyond the oxidative capacity leads to accumulation of intramuscular triglycerides (IMTG), which have been linked to insulin resistance (4). In turn, insulin-mediated glucose uptake is diminished, causing elevated plasma glucose levels. Recent work in BAT, a tissue originally thought to be minimally existent in adults, has sparked interest as a potential therapeutic role in combating obesity and T2DM (5). Like in skeletal muscle, glucose uptake in BAT is mediated by GLUT4 (6); thus, BAT is a tissue of interest in developing insulin sensitizing drugs. BAT is also a thermoregulator; increased density of mitochondria in BAT produce more energy via substrate oxidation, which is dissipated as heat in the tissue (7). The liver is the central organ for glucose homeostasis (8). Insulin resistance acts as positive feedback by increasing the rate of gluconeogenesis when plasma glucose is already high. The liver is also a major site for FA oxidation, however, high intracellular lipid content will blunt the oxidative pathway resulting in more storage of FAs, and eventually release of VLDLs, thus increasing peripheral FFA levels (9). Finally, a number of studies have focused on interplay between obesity, diabetes and secondary effects on substrate metabolism in the heart. In previous publications, we have demonstrated that decreased glucose utilization in the ZDF rat is associated with lowered expression of GLUT4 in the heart, as well as the effect of RGZ to increase glucose utilization as well as FA oxidation in ZDF rat hearts (10, 11). In isolated ZDF rat hearts, greater concentration of FA transport proteins at the plasma membrane is associated with greater flux of FA into the tissue (12). However, the two factors influencing increased FA transport (high circulating FFA levels and increased expression of transport proteins) are rarely examined independently.

In light of the highly interconnected and coordinated nature of substrate metabolism, and its failure in disease, an understanding of intrinsic and extrinsic metabolic mechanisms in affected tissues is critical to devising therapeutic approaches for T2DM. Thus, the objective of this work was to characterize *in vivo* metabolic alterations in multiple tissues affected by T2DM. In addition, the secondary goal of the present work was to assess multi-tissue metabolic efficacy of the PPARγ agonist rosiglitazone (RGZ). PPARγ agonists of the thiazolidinedione class have been shown to improve whole body insulin sensitivity (13). We

have previously assessed the effects of RGZ on myocardial fatty acid metabolism (10). However the efficacy of PPARγ agonists on both glucose and FA metabolism in affected tissues has yet to be determined *in vivo*. To that end, in our current work we aim to first, assess the metabolic phenotype of glucose and FA metabolism in the liver, heart, skeletal muscle and BAT of non-diabetic and diabetic rats, and second, assess the effects of RGZ on glucose and FA metabolism in affected tissues.

Methods and Procedures

All chemicals were purchased from Aldrich Chemical Co. (St. Louis, MO). Radioactive samples were counted on an 8000 γ-counter (Beckman Coulter, Indianapolis, IN). PET radiotracers [^{18}F]FDG and [^{11}C]Palmitate, metabolic analogs of glucose and FA respectively, were produced at the Washington University Cyclotron Facility.

Animal Models and Preparation

Metabolic imaging studies utilized one group of Lean Zucker rats and three groups of Zucker Diabetic Fatty (ZDF): Lean (N=6) and one group of ZDF (N=6) rats were studied at 14 weeks to characterize alterations in metabolic substrate preference (denoted as “No Treatment” baseline groups); one group of ZDF rats (N=6) was studied at age of 19 weeks; and one group of ZDF rats (N=6) was treated with rosiglitazone (RGZ; 4 mg/kg/day; N=6) for 5 weeks starting at the age of 14 weeks and studied at age of 19 weeks (denoted as “Treatment” group). Small-animal PET was performed on all animals at either 14 or 19 weeks of age as indicated above. A separate group of rats were used to characterize arterial and portal vein (PV) tracer kinetics for use in quantification of the liver dual input function (LDIF) as described in the supplemental material. All animals were fed Purina Constant Nutrition 5008 (Purina, St. Louis, MO) diet throughout the study, with the treated group receiving the RGZ drug in its diet. Animals were fasted overnight prior to imaging. All studies were approved by the Washington University Animal Studies Committee in agreement with the Guidelines for the Care and Use of Laboratory Animals.

Pre-Clinical PET Imaging Protocol

Dynamic PET acquisition was started after a bolus injection of radiopharmaceutical via tail vein. Rats were anesthetized by inhalation of 2–2.5% Isoflurane administered via an induction chamber. Small-animal PET was performed on either the microPET Inveon or Focus-220 (14) (Siemens Inc., Malvern, PA). Scanners were cross-calibrated to ensure reliability of the data. Body temperature was maintained at 37°C by a circulating water blanket and heat lamp. In addition heart and respiratory rates were monitored throughout the imaging session. The session began with a 20-minute acquisition with [^{11}C]Palmitate (22.2–29.6 MBq) to quantify tissue fatty acid metabolism followed by a 60-minute scan with [^{18}F]FDG (18.5–29.6 MBq) to quantify tissue glucose metabolism. During each imaging session, 5–6 arterial whole-blood samples were taken from the femoral artery to measure plasma glycosylated hemoglobin (HbA1c) and glucose (5 μL), insulin (5 μL), and fatty acid (FFA; 20 μL) levels, as well as to correct for the presence of $^{11}CO_2$ metabolites (15).

Image Processing

Images from PET scans were reconstructed using filtered back-projection algorithm. The images from all the frames were summed into a single image and regions of interest (ROIs) were drawn on the right lobe of the liver to obtain the liver time activity curve (5), on left intercostal muscle to obtain the muscle time activity curve (5), and on interscapular fat to obtain the BAT TAC. The ROIs from the summed image of first tracer imaging were subsequently transferred to the successive image scans with other tracers to maintain consistent ROIs.

Image Quantification

In reporting tissue metabolic parameters a distinction is made between intrinsic and extrinsic measures. Intrinsic metabolic parameters refer to the intrinsic capacity of the tissue to metabolize a given substrate and are reported as rates whereas the extrinsic metabolic parameters take into account peripheral concentration of a given substrate to yield the flux into tissue.

Derivation of the Input Function

The arterial input function (AIF) was reconstructed using the hybrid input blood sampling algorithm (HIBS), as described previously (16). HIBS-derived input functions were corrected for ^{11}C metabolites, as described previously (15). To assess liver metabolism, the LDIF was determined by estimating arterial and PV flow fractions. The LDIF is thus a weighted sum of the AIF and the estimated PV kinetics weighted by their respective flow fractions. A detailed description of the LDIF quantification is shown in the Supplementary Methods.

Brown Fat and Muscle Substrate Metabolism

FA Metabolism—The compartmental model describing [^{11}C]Palmitate kinetics in brown fat and muscle is shown in Figure 1A. The model consisted of one vascular compartment and two tissue compartments $C_1(t)$ and $C_2(t)$, representing the activity in the interstitial and cytosolic space, and slow-turnover lipid pool, respectively. The rate constants denoted by K_1 (mL/min/g), k_2 (/min), k_3 (/min) and k_4 (/min) represent the forward transport, back-diffusion into plasma, FA esterification, and lipolysis, respectively. The disadvantage of this model is that the oxidative flux and clearance are lumped into the clearance parameter k_2; the rationale is that both the clearance of [^{11}C]Palmitate and oxidative metabolites of [^{11}C]Palmitate are cleared through the periphery. Higher order models (3 tissue compartments, 5 parameters) were tested; however, they did not show statistical need. The kinetic parameters K_1, k_2, k_3 k_4 were determined by optimizing the model against the tissue TAC using a non-linear least squares approach formulated in MATLAB (MathWorks Inc., Natick, MA). The tracer uptakes and fluxes were estimated using steady state analysis. Here, we report three measures of FA metabolism: K_1, the transport rate constant, FAE_{int}, the intrinsic FA esterification rate, and FAE_{ext}, the extrinsic FA esterification rate (see Supplementary Methods). Intrinsic measures of FA metabolism, FAE_{int}, represent the uptake rate-constant of FA destined for esterification whereas FAE_{ext} represents the flux destined for esterification.

Glucose Metabolism

A three-compartment, three-parameter model, i.e. omitting k_4, was used to describe the kinetics of [^{18}F]FDG, where $C_1(t)$ and $C_2(t)$ represent the unphosphorylated and phosphorylated [^{18}F]FDG compartments respectively (17). We chose to omit k_4, the dephosphorylation rate constant, when estimating parameters in muscle and BAT due to the very low concentrations of glucose-6 phosphatase, the hydrolyzing enzyme involved in dephosphorylation of G6P (18). To estimate the three parameters K_1, k_2, and k_3, 60 minutes of [^{18}F]FDG data were optimized against the tissue TAC. For glucose metabolism, we also show three estimates: K_1, glucose transport rate constant, GUR_{int}, the intrinsic glucose utilization rate, and GUR_{ext}, the extrinsic glucose utilization rate (see Supplemental Methods).

Cardiac Substrate Metabolism

A four-compartment model shown in Figure 1B was used to estimate [^{11}C]Palmitate kinetics in the heart as shown previously in treated ZDF rats (10). The model is able to delineate FA esterification and oxidation pathways. Consequently intrinsic and extrinsic FA utilization (FAU_{int}, FAU_{ext}) in the heart is a combination of both oxidized and stored FAs. Measures of glucose utilization in the heart were estimated as described previously (11) using a graphical analysis approach (19) to derive GUR_{int}. In the subsequent data, we will consistently use the labels GUR_{ext} and GUR_{int} to represent the extrinsic and intrinsic glucose uptake rate, respectively, given we have distinguished their meanings in each tissue.

Hepatic Substrate Metabolism

FA Metabolism—The two tissue compartmental model in Figure 1A was used to describe [^{11}C]Palmitate kinetics in the liver. A similar compartmental model was used before to describe kinetics of fatty acid analog tracer in the liver (20). The first tissue compartment C_1 represents the unmetabolized [^{11}C]Palmitate and the second compartment C_2 represents the esterification of [^{11}C]Palmitate. The rate constants for the compartmental model are denoted by K_1 (mL/min/g), k_2 (/min), k_3 (/min) and k_4 (/min). FAE is defined as is for brown fat and muscle. More detail of the computations can be found in the Supplemental Methods.

Glucose Metabolism—To describe [^{18}F]FDG kinetics in liver, several kinetic models were evaluated. Specifically we evaluated 3 variations of the typical 2-compartment model: A) a 3-parameters (3P) model depicting trapping of [^{18}F]FDG metabolites; B) a 4-parameter (4P) model depicting phosphorylation and dephosphorylation of [^{18}F]FDG and ^{18}FDG6P, respectively; and C) based on a recent report on potential downstream metabolism of [^{18}F]FDG (21), a 5-parameter (5P) model was evaluated to account for metabolism beyond [^{18}F]FDG6P. However, statistical analysis suggested that the standard two-compartment 3P was found to be sufficient to describe [^{18}F]FDG kinetics in the liver (data not shown). Overall, we did not observe significant differences in [^{18}F]FDG metabolism in the liver between lean and diabetic rats as well as in response to treatment. For brevity, [^{18}F]FDG liver data are not summarized.

Data Optimization

The Levenberg-Marquardt algorithm was used to minimize the Weighted Residual Sum of Squares (WRSS) with the model optimized against the dynamic PET data. The weights used were proportional to square root of the ratio of scan duration to tissue ROI activity.

Statistical Analysis

All measures were expressed as mean ± SEM, except where noted otherwise. An unpaired t-test was used to determine differences between ZDF and lean rats at baseline (i.e. 14W) and between treated and untreated ZDF rats. A P-value less than 0.05 was considered significant.

RESULTS

Plasma Substrate Levels and Animal Characteristics

Untreated ZDF rats were characteristically hyperglycemic, as shown by elevated plasma glucose and glycosylated hemoglobin levels compared to lean rats as shown in Table 1. Treatment with RGZ decreased HbA1c levels by 40% ($P<0.001$), but we did not see improvement in fasting plasma glucose levels potentially due to effects of anesthesia. In the untreated group, ZDF rats exhibited lower heart rates than Lean rats. Plasma FFA levels were significantly higher ($P<0.05$) in untreated ZDF rats compared to leans, while treated ZDF rats showed no significant change in circulating FFAs. Treated rats gained more ($P<0.001$) weight than untreated rats.

Brown Adipose Tissue

Baseline Metabolic Phenotype—Untreated ZDF rats have significantly diminished ($P<0.05$) transport of glucose compared to leans as evident in K_1 (Figure 2A). While the intrinsic glucose uptake rate-constant was not significantly lower in ZDF rats, ZDF rats tended to have a lower GUR_{int} (Figure 2B). When taking into account peripheral glucose levels, there were no significant differences in GUR_{ext} between lean and ZDF rats (Figure 2C). On the other hand, the uptake of [^{11}C]Palmitate as estimated by K_1 was significantly lower in ZDF rats ($P<0.001$) (Figure 2A) while no significant differences in intrinsic measures of FAE were observed between the two groups (Figure 2B). Primarily due to higher peripheral levels of FA, extrinsic measures of FAE tended to be higher in ZDF rats, though the results did not reach significance (Figure 2C).

Effects of Treatment—RGZ-treated rats exhibited significantly higher glucose and FA transport as shown in Figure 2D; however, there were no significant differences in intrinsic and extrinsic measures of glucose and FA uptake rate and esterification, although treatment with RGZ tended to reduce FAE (Figure 2E–2F).

Skeletal Muscle Substrate Metabolism

Baseline Metabolic Phenotype—At baseline, ZDF rats exhibited significantly lower transport of [^{18}F]FDG compared to lean rats (Figure 3A), consistent with the diabetic phenotype. However, due to higher peripheral concentration of glucose, the overall flux of glucose is higher in ZDF rats than Lean rats (Figure 3C). Similarly due to higher presence of

FFA in the periphery, extrinsic measures of FA flux tended to be higher in ZDF rats than Lean rats, though the results did not reach significance.

Effects of Treatment—Treatment with PPARγ agonist tended to increase intrinsic measures of glucose uptake (Figure 3A) while diminishing intrinsic measures of FA uptake (Figure 3E). In particular, both FAE and FAE_{UpR} were noticeably lower in RGZ-treated ZDF rats.

Cardiac Substrate Metabolism

Baseline Metabolic Phenotype—ZDF rats exhibit significantly lower intrinsic uptake of glucose, while, in parallel, ZDF rats exhibit significantly higher intrinsic rates of FAU (Figure 4A). When taking into account peripheral levels of glucose and FFA, the higher concentration of glucose in ZDF rats annuls differences in GUR_{ext} and exacerbates flux of FA into the myocardium (Figure 4B).

Effects of Treatment—Overall, treatment with RGZ resulted in significantly higher ($P<0.05$) uptake rate-constant of glucose (Figure 4C) with significant reduction in both intrinsic ($P<0.01$) and extrinsic ($P<0.01$) measures of FAU (Figure 4D).

Liver Substrate Metabolism

No significant changes were observed in GUR_{int} or GUR_{ext} in the liver between Lean and ZDF rats or following treatment (data not shown). Similarly, intrinsic measures of FA metabolism were not significantly different between the groups (Figure 5A). In contrast, ZDF rats exhibited significantly higher utilization of FA destined toward FAE storage, presumably as TG, due to overall higher peripheral concentration of FFA (Figure 5B–5C). Since RGZ did not cause a significant reduction in peripheral FA concentrations, extrinsic measures of FA utilization did not change following treatment. Interestingly, the flux of [^{11}C]Palmitate destined to FAE was significantly lower following RGZ therapy (Figure 5F).

DISCUSSION

Systemic alterations in peripheral metabolism is one of the hallmarks of obesity and T2DM with current drugs and others in the pipeline targeting key pivots of substrate metabolism. The objective of this work, therefore, was to non-invasively quantify glucose and FA metabolism in tissues known to be affected in T2DM; in particular, BAT, skeletal muscle, heart, and the liver of lean and obese diabetic rats. In addition, we sought to assess the response of above-mentioned tissues to PPARγ therapy. Previous studies have characterized metabolic alterations independently in muscle (12, 22, 23) or heart (10, 11). However, the simultaneous contribution of individual tissues has scarcely been reported. Guiducci et. al (24) recently characterized the contribution of blood flow and tissue clearance on extrinsic measures of FDG metabolism in multiple tissues. In contract, in this work, we characterize both glucose and FA substrate metabolism in multiple tissues. Finally, as mentioned earlier, we make a distinction between intrinsic measures of substrate metabolism and extrinsic measures of flux, with the former being independent of peripheral substrate concentrations.

In BAT and muscle, we observed a reduction in glucose transport (K_1) in diabetic rats. The intrinsic glucose uptake rate-constant, GUR_{int}, was significantly reduced in diabetic hearts, but unchanged in BAT and muscle suggesting an uncoupling of transport and phosphorylation processes in muscle and BAT. Interestingly, Williams et al (25) reported no differences in K_1 or GUR_{int} in skeletal muscle in a human PET study of obese and T2DM individuals using similar modeling methods. When examining the extrinsic uptake of glucose, GUR_{ext}, we observed no differences in GUR_{ext} in BAT and heart between lean and diabetic rats due to the higher peripheral levels of glucose which masked the lower GUR_{int} in diabetic rats. However, diabetic rats exhibited higher GUR_{ext} in muscle than lean rats in agreement with previous reports (24, 26, 27). Thus, while the intrinsic cellular mechanisms in muscle, such as glucose transport as captured through the K_1 parameter, blunt glucose uptake, the higher peripheral concentration of glucose resulted in overall greater flux of glucose into tissue. In the liver, we did not observe differences in [^{18}F]FDG kinetics between lean and ZDF rats, most likely due limitations in downstream metabolism of [^{18}F]FDG and due to high levels of glucose-6-phosphotase which result in clearance of [^{18}F]FDG. Overall, our data indicate that ZDF rats have an innate deficiency in glucose transport in muscle, BAT, and heart, which is attributed to down-regulation of GLUT transporters in the diabetic state (11, 12, 28).

RGZ improved insulin sensitivity more so in BAT than in muscle as seen by the significant increase in K_1, although glucose transport tended to be higher following therapy in muscle as well. Indeed, insulin has been shown to significantly increase glucose uptake in BAT (29). Moreover, tissue-specific knockout of insulin receptors in BAT has shown to promote a diabetic phonotype (30). We did not observe significant changes in GUR_{int} and GUR_{ext} in treated rats consistent with that found in humans (31). In addition, GUR_{int} significantly improved in heart, while the increase in GUR_{ext} trend did not reach significance. These results demonstrate the effects of PPARγ agonists on peripheral tissues and are in accord with previous reports on the efficacy of this drug class (28, 32–34). One possible mechanism of TZDs is increased expression of insulin sensitive genes resulting in translocation of GLUT4 (10, 13). GLUT4 translocation will lead to increased glucose disposal and a net decrease in peripheral glucose levels. We did not observe changes in glucose levels following therapy despite lower HbA1C levels, possibly due to the effects of anesthesia. However, our data clearly demonstrate therapeutic response of RGZ resulting in increased glucose transport (K_1), attributed to GLUT4 translocation as we have demonstrated previously (11).

Increased fatty acid uptake has been implicated in the pathogenesis of the metabolic alterations that accompany T2DM and obesity (9). Our results show that ZDF rats have higher circulating FFA levels compared to leans. Interestingly, ZDF rats had decreased transport of [^{11}C]Palmitate compared to leans in both BAT and muscle. Previous studies by Bonen *et al* and Luiken *et al* (12, 23) have shown that both increased FFAs and greater FAT/CD36 protein content at the cell membrane account for greater FA transport in fat, muscle, and heart of ZDF rats. Conversely, Blaak *et al* report of impairment in FA uptake in obese and T2DM humans (35). Our data suggest that the amount of intracellular FA represented by the concentration in compartment 1 (Figure 1A) would be similar in lean and

ZDF rats given the high plasma FFA levels. When considering the esterification of FAs, ZDF rats tended to have both greater intrinsic and extrinsic FAE in muscle, BAT, and heart, although no statistical significance could be reached for estimates in BAT and muscle. We assume that the increased FAE is not just attributed to elevated plasma FFA concentrations, but also to an intracellular mechanism that partitions more FA toward storage. Thus, the actual metabolic impairment may be how FAs are handled once in the cell, which in ZDF rats, seems to be a shift toward increased FA esterification. One theory is that tissues are operating beyond their oxidative capacity due to lowered number of mitochondira and/or higher flux and therefore store FAs at a higher rate to compensate for the increased availability of lipids (22). The rise of intramuscular triglyceride levels in turn impairs muscle glucose uptake (4).

The effect of TZDs on FA metabolism has also been well studied in humans and animal models of diabetes. Coort and colleagues showed that RGZ increased FA uptake in adipose tissue but not in muscle or heart membrane vesicles in Zucker rats, due in part to greater FAT/CD36 and FATP1 concentration at the cell membrane (36). Palmitate oxidation in skeletal muscle was shown to increase in healthy rats but not ZDFs treated with RGZ (37, 38). Our data clearly demonstrate a significant increase in FA transport in BAT with a nominal increase in muscle following RGZ. Both intrinsic and extrinsic measures of FAE tended to be lower in muscle and BAT. Similarly, overall FA utilization was significantly reduced in the heart. We have previously shown that RGZ inhibits FA oxidation in the heart which we attributed to blunt reduction in expression of genes encoding MCAD and FATP-I (10). In the liver, we found that RGZ treatment caused significant ($P<0.05$) reduction in fatty acid esterification, in agreement with the reduced lipid storage with rosiglitazone therapy in rats (39). Taken together, our data suggest that RGZ acts by reducing storage of exogenous FA in lipid pools, possibly by initiating a remodeling process that increases lipolysis of stored FA in non-adipose tissues and increases the efficiency of adipose tissue to store fat by increasing the number but decreasing the size of adipocytes (40).

In this study, we reported the metabolic dysfunction seen in the ZDF rat, an obese animal model of T2DM, and the effect of RGZ on improving insulin sensitivity and FA utilization in multiple affected tissues using pre-clinical PET and quantitative modeling. Glucose transport is impaired in the ZDF rat but is ameliorated by RGZ in heart, skeletal muscle, and brown fat. There is also a tendency toward increased esterification of FAs in these tissues, the severity of which was improved with RGZ therapy in a tissue specific manner. Consequently, we have emphasized the importance of examining multiple tissues and using appropriate physiologic models to understand the biological mechanisms that arise in T2DM and during therapy. These developments highlight the potential to screen therapeutic interventions for diabetes, obesity, and metabolic diseases classified under the umbrella “metabolic syndrome” as well as to characterize the progression of diabetes and the interplay with cardiovascular disease.

Acknowledgments

SN and SR analyzed and interpreted the data and contributed to writing the manuscript. KS analyzed, interpreted, contributed to writing the manuscript, and approved the final version for publication. This work was supported by NIH grant No. 5R01DK085298. We would like to thank the Preclinical PET/CT Imaging Facility at Washington

University School of Medicine for technical support, as well as the Washington University Cyclotron Facility for production of radiopharmaceuticals. The work utilized core-services provided by the Diabetes Research Center (DRC), Grant No. P60DK020579, and the Nutrition Obesity Research Center (NORC), Grant No. P30DK056341.

References

1. Kahn BB, Flier JS. Obesity and insulin resistance. J Clin Invest. 2000; 106(4):473–81. [PubMed: 10953022]
2. Flier JS. Diabetes. The missing link with obesity? Nature. 2001; 409(6818):292–3. [PubMed: 11201721]
3. Wilson PW. Diabetes mellitus and coronary heart disease. Endocrinol Metab Clin North Am. 2001; 30(4):857–81. [PubMed: 11727403]
4. Phillips DI, Caddy S, Ilic V, Fielding BA, Frayn KN, Borthwick AC, et al. Intramuscular triglyceride and muscle insulin sensitivity: evidence for a relationship in nondiabetic subjects. Metabolism. 1996; 45(8):947–50. [PubMed: 8769349]
5. Fruhbeck G, Becerril S, Sainz N, Garrastachu P, Garcia-Velloso MJ. BAT: a new target for human obesity? Trends Pharmacol Sci. 2009; 30(8):387–96. [PubMed: 19595466]
6. Kawashita NH, Brito MN, Brito SR, Moura MA, Festuccia WT, Garofalo MA, et al. Glucose uptake, glucose transporter GLUT4, and glycolytic enzymes in brown adipose tissue from rats adapted to a high-protein diet. Metabolism. 2002; 51(11):1501–5. [PubMed: 12404205]
7. Nicholls DG, Locke RM. Thermogenic mechanisms in brown fat. Physiol Rev. 1984; 64(1):1–64. [PubMed: 6320232]
8. Pilkis SJ, Granner DK. Molecular physiology of the regulation of hepatic gluconeogenesis and glycolysis. Annu Rev Physiol. 1992; 54:885–909. [PubMed: 1562196]
9. McGarry JD. Banting lecture 2001: dysregulation of fatty acid metabolism in the etiology of type 2 diabetes. Diabetes. 2002; 51(1):7–18. [PubMed: 11756317]
10. Shoghi KI, Finck BN, Schechtman KB, Sharp T, Herrero P, Gropler RJ, et al. In vivo metabolic phenotyping of myocardial substrate metabolism in rodents: differential efficacy of metformin and rosiglitazone monotherapy. Circ Cardiovasc Imaging. 2009; 2(5):373–81. [PubMed: 19808625]
11. Shoghi KI, Gropler RJ, Sharp T, Herrero P, Fettig N, Su Y, et al. Time Course of Alterations in Myocardial Glucose Utilization in the Zucker Diabetic Fatty Rat with Correlation to Gene Expression of Glucose Transporters: A Small-Animal PET Investigation. J Nucl Med. 2008; 49(8): 1320–7. [PubMed: 18632819]
12. Bonen A, Holloway GP, Tandon NN, Han XX, McFarlan J, Glatz JF, et al. Cardiac and skeletal muscle fatty acid transport and transporters and triacylglycerol and fatty acid oxidation in lean and Zucker diabetic fatty rats. Am J Physiol Regul Integr Comp Physiol. 2009; 297(4):R1202–12. [PubMed: 19675275]
13. Day C. Thiazolidinediones: a new class of antidiabetic drugs. Diabet Med. 1999; 16(3):179–92. [PubMed: 10227562]
14. Tai Y-C, Ruangma A, Rowland D, Siegel S, Newport DF, Chow PL, et al. Performance Evaluation of the microPET Focus: A Third-Generation microPET Scanner Dedicated to Animal Imaging. J Nucl Med. 2005; 46(3):455–63. [PubMed: 15750159]
15. Dence, CS.; Herrero, P.; Schwarz, SW.; Mach, RH.; Gropler, RJ.; Welch, MJ., et al. Methods in Enzymology. Academic Press; 2004. Imaging Myocardium Enzymatic Pathways with Carbon-11 Radiotracers; p. 286-315.
16. Shoghi K. Hybrid image-blood-sampling input function with a Bezier linker for quantification of microPET data. J NUCL MED MEETING ABSTRACTS. 2007; 48:402P-b. MeetingAbstracts_2.
17. Williams KV, Bertoldo A, Mattioni B, Price JC, Cobelli C, Kelley DE. Glucose transport and phosphorylation in skeletal muscle in obesity: insight from a muscle-specific positron emission tomography model. J Clin Endocrinol Metab. 2003; 88(3):1271–9. [PubMed: 12629118]
18. Ferre P, Leturque A, Burnol AF, Penicaud L, Girard J. A method to quantify glucose utilization in vivo in skeletal muscle and white adipose tissue of the anaesthetized rat. Biochem J. 1985; 228(1): 103–10. [PubMed: 3890836]

19. Patlak CS, Blasberg RG. Graphical evaluation of blood-to-brain transfer constants from multiple-time uptake data. Generalizations. J Cereb Blood Flow Metab. 1985; 5(4):584–90. [PubMed: 4055928]
20. DeGrado TR, Wang S, Rockey DC. Preliminary Evaluation of 15-[18F]Fluoro-3-oxa-pentadecanoate as a PET Tracer of Hepatic Fatty Acid Oxidation. Journal of Nuclear Medicine. 2000; 41(10):1727–36. [PubMed: 11038005]
21. Southworth R, Parry CR, Parkes HG, Medina RA, Garlick PB. Tissue-specific differences in 2-fluoro-2-deoxyglucose metabolism beyond FDG-6-P: a 19F NMR spectroscopy study in the rat. NMR in Biomedicine. 2003; 16(8):494–502. [PubMed: 14696007]
22. Holloway GP, Benton CR, Mullen KL, Yoshida Y, Snook LA, Han XX, et al. In obese rat muscle transport of palmitate is increased and is channeled to triacylglycerol storage despite an increase in mitochondrial palmitate oxidation. Am J Physiol Endocrinol Metab. 2009; 296(4):E738–47. [PubMed: 19141681]
23. Luiken JJ, Arumugam Y, Dyck DJ, Bell RC, Pelsers MM, Turcotte LP, et al. Increased rates of fatty acid uptake and plasmalemmal fatty acid transporters in obese Zucker rats. J Biol Chem. 2001; 276(44):40567–73. [PubMed: 11504711]
24. Guiducci L, Liistro T, Burchielli S, Panetta D, Bonora D, Di Cecco P, et al. Contribution of organ blood flow, intrinsic tissue clearance and glycaemia to the regulation of glucose use in obese and type 2 diabetic rats: A PET study. Nutrition, Metabolism and Cardiovascular Diseases. 2011; 21(9):726–32.
25. Williams KV, Price JC, Kelley DE. Interactions of impaired glucose transport and phosphorylation in skeletal muscle insulin resistance: a dose-response assessment using positron emission tomography. Diabetes. 2001; 50(9):2069–79. [PubMed: 11522673]
26. Leonard BL, Watson RN, Loomes KM, Phillips AR, Cooper GJ. Insulin resistance in the Zucker diabetic fatty rat: a metabolic characterisation of obese and lean phenotypes. Acta Diabetol. 2005; 42(4):162–70. [PubMed: 16382303]
27. Nawano M, Oku A, Ueta K, Umebayashi I, Ishirahara T, Arakawa K, et al. Hyperglycemia contributes insulin resistance in hepatic and adipose tissue but not skeletal muscle of ZDF rats. Am J Physiol Endocrinol Metab. 2000; 278(3):E535–43. [PubMed: 10710509]
28. Kramer D, Shapiro R, Adler A, Bush E, Rondinone CM. Insulin-sensitizing effect of rosiglitazone (BRL-49653) by regulation of glucose transporters in muscle and fat of Zucker rats. Metabolism. 2001; 50(11):1294–300. [PubMed: 11699047]
29. Hardman MJ, Hull D. The action of insulin on brown adipose tissue in vivo. J Physiol. 1972; 221(1):85–92. [PubMed: 5016995]
30. Guerra C, Navarro P, Valverde AM, Arribas M, Bruning J, Kozak LP, et al. Brown adipose tissue-specific insulin receptor knockout shows diabetic phenotype without insulin resistance. J Clin Invest. 2001; 108(8):1205–13. [PubMed: 11602628]
31. Iozzo P, Hallsten K, Oikonen V, Virtanen KA, Parkkola R, Kemppainen J, et al. Effects of metformin and rosiglitazone monotherapy on insulin-mediated hepatic glucose uptake and their relation to visceral fat in type 2 diabetes. Diabetes Care. 2003; 26(7):2069–74. [PubMed: 12832315]
32. Cypess AM, Kahn CR. Brown fat as a therapy for obesity and diabetes. Curr Opin Endocrinol Diabetes Obes. 2010; 17(2):143–9. [PubMed: 20160646]
33. Hallsten K, Virtanen KA, Lonnqvist F, Janatuinen T, Turiceanu M, Ronnemaa T, et al. Enhancement of insulin-stimulated myocardial glucose uptake in patients with Type 2 diabetes treated with rosiglitazone. Diabet Med. 2004; 21(12):1280–7. [PubMed: 15569129]
34. Hofmann C, Lorenz K, Colca JR. Glucose transport deficiency in diabetic animals is corrected by treatment with the oral antihyperglycemic agent pioglitazone. Endocrinology. 1991; 129(4):1915–25. [PubMed: 1915075]
35. Blaak EE. Basic disturbances in skeletal muscle fatty acid metabolism in obesity and type 2 diabetes mellitus. Proc Nutr Soc. 2004; 63(2):323–30. [PubMed: 15294050]
36. Coort SL, Coumans WA, Bonen A, van der Vusse GJ, Glatz JF, Luiken JJ. Divergent effects of rosiglitazone on protein-mediated fatty acid uptake in adipose and in muscle tissues of Zucker rats. J Lipid Res. 2005; 46(6):1295–302. [PubMed: 15772429]

37. Benton CR, Holloway GP, Campbell SE, Yoshida Y, Tandon NN, Glatz JF, et al. Rosiglitazone increases fatty acid oxidation and fatty acid translocase (FAT/CD36) but not carnitine palmitoyltransferase I in rat muscle mitochondria. J Physiol. 2008; 586(6):1755–66. [PubMed: 18238811]

38. Sreenan S, Keck S, Fuller T, Cockburn B, Burant CF. Effects of troglitazone on substrate storage and utilization in insulin-resistant rats. Am J Physiol. 1999; 276(6 Pt 1):E1119–29. [PubMed: 10362626]

39. Lessard SJ, Rivas DA, Chen ZP, Bonen A, Febbraio MA, Reeder DW, et al. Tissue-specific effects of rosiglitazone and exercise in the treatment of lipid-induced insulin resistance. Diabetes. 2007; 56(7):1856–64. [PubMed: 17440174]

40. de Souza CJ, Eckhardt M, Gagen K, Dong M, Chen W, Laurent D, et al. Effects of pioglitazone on adipose tissue remodeling within the setting of obesity and insulin resistance. Diabetes. 2001; 50(8):1863–71. [PubMed: 11473050]

What is already known about this subject?

- Glucose and fatty acid (FA) metabolism are impaired in Type 2 Diabetes Mellitus (T2DM)
- Deficiencies in insulin signaling result in greater reliance on FA metabolism
- Insulin sensitizing drugs such as rosiglitazone have shown to to normalize glucose uptake

What does this study add?

- We demonstrate glucose and FA metabolic dysfunction in ZDF rats in-vivo in multiple tissues using preclinical PET imaging and kinetic modeling.
- We demonstrate the effects of rosiglitazone on insulin sensitivity and FA utilization in multiple affected tissues in-vivo
- We demonstrate the importance of peripheral tissues in substrate disposal and the utility of quantitative preclinical imaging to assess the efficacy of anti-diabetic drugs

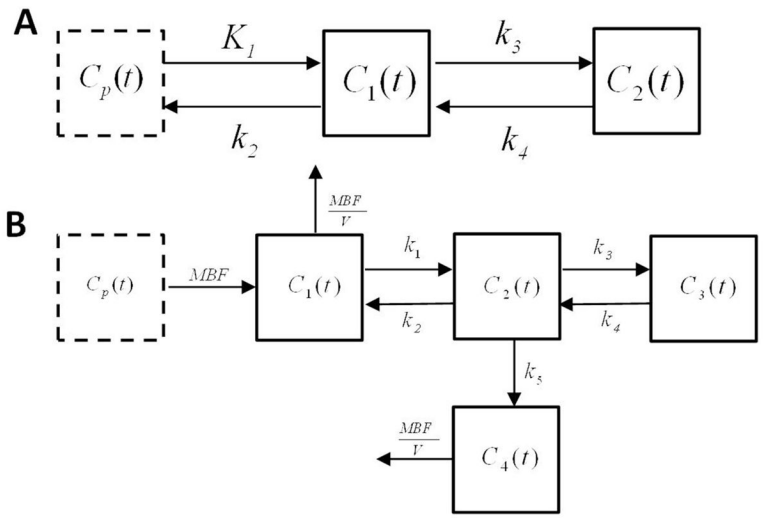

Figure 1.

(A)Two-compartment model with plasma input function and rate constants k_1 through k_4 describing [^{18}F]FDG and [^{11}C]Palmitate kinetics in brown fat, muscle and liver. (B) Four-compartment model with plasma input function and rate constants k_1 through k_5 for [^{11}C]Palmitate kinetics in heart.

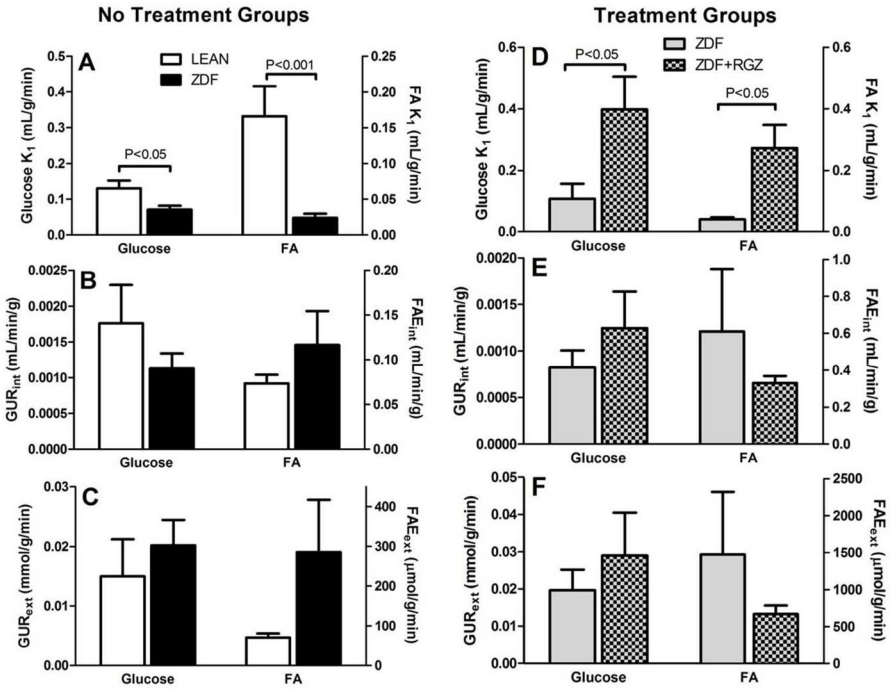

Figure 2.

Intrinsic and extrinsic measures of [^{18}F]FDG and [^{11}C]Palmitate uptake and metabolism in brown adipose without treatment (left column) and with PPARγ treatment (right column). Top row represents fractional transport of [^{18}F]FDG and [^{11}C]Palmitate; middle row depicts measures of [^{18}F]FDG uptake rate-constant and intrinsic FAE rate; and bottom row represents extrinsic measures of [^{18}F]FDG uptake and FAE flux. Note the dual Y-axis with left axis representing glucose parameters and right axis representing FA parameters.

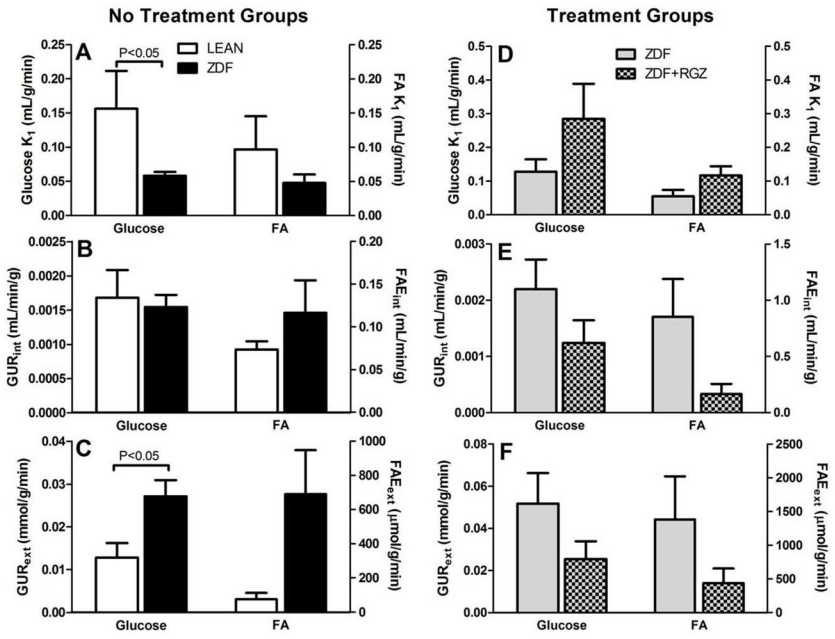

Figure 3.

Intrinsic and extrinsic measures of [^{18}F]FDG and [^{11}C]Palmitate uptake and metabolism in muscle without treatment (left column) and with PPARγ treatment (right column). Top row represents fractional transport of [^{18}F]FDG and [^{11}C]Palmitate; middle row depicts measures of [^{18}F]FDG uptake rate-constant and intrinsic FAE rate; and bottom row represents extrinsic measures of [^{18}F]FDG uptake and FAE flux. Note the dual Y-axis with left axis representing glucose parameters and right axis representing FA parameters.

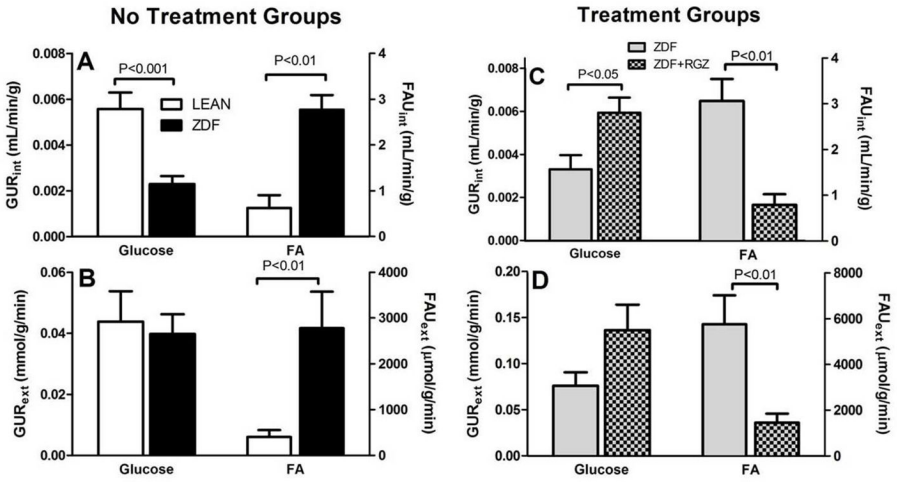

Figure 4.

Intrinsic and extrinsic measures of [^{18}F]FDG and [^{11}C]Palmitate uptake and metabolism in heart without treatment (left column) and with PPARγ treatment (right column). Top row depicts intrinsic measures of [^{18}F]FDG uptake and intrinsic FAU; bottom row represents extrinsic measures of [^{18}F]FDG uptake and FAU. Note the dual Y-axis with left axis representing glucose parameters and right axis representing FA parameters.

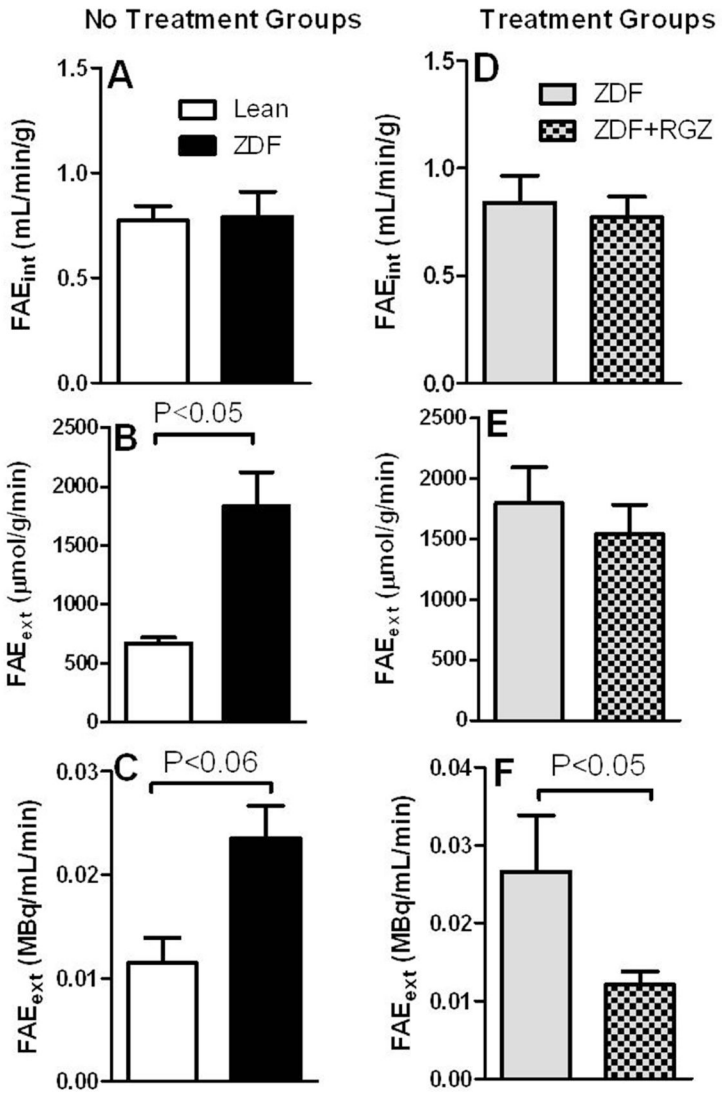

Figure 5.

Intrinsic and extrinsic fatty acid esterification (FAE) in the liver for untreated (left column) and with PPARγ treatment (right column) showing the significant reduction in the rosiglitazone treated rats. Error bars denote SEM. Top row shows intrinsic FAE rate, FAE flux is calculated using both plasma FFA levels (middle row) and [^{11}C]Palmitate plasma activity (bottom row).

Table 1

Animal demographics and plasma substrate levels

	No Treatment		Treatment	
	Lean	**ZDF**	**ZDF**	**ZDF+RGZ**
Weight (g)	306±11	322±18	344±21	513±48[b]
HR (bpm)	246±21	215±26[a]	198±15	209±3
HbA1C (%)	3.33±0.12	7.69±0.56[a]	7.38±0.73	4.40±0.70[b]
Insulin (μU/mL)	11.4±3.77	34.21±17.7[a]	18±11	28.1±15.8
Glucose (mM)	7.52±2.18	17.6±4.9[a]	23±2.5	21.80±7.1
FFA (μmol/L)	826±301	2320±1134[a]	1920±891	2029±642

[a] P<0.05 Significantly different than Leans

[b] P<0.05 Significantly different than untreated ZDF